

# A Robust Approach to Minimizing $\mathbf{H}(\text{div})$ -Dominated Functionals in an $\mathbf{H}^1$ -Conforming Finite Element Space<sup>†</sup>

Travis M. Austin<sup>1,\*</sup>, Thomas A. Manteuffel<sup>2</sup>, and Steve McCormick<sup>2</sup>

<sup>1</sup> *MS B284, T-7, Los Alamos National Laboratory, Los Alamos, NM 87545*

<sup>2</sup> *Dept. of Applied Mathematics, Campus Box 526, University of Colorado at Boulder, Boulder, CO 80309-0526*

## SUMMARY

The standard multigrid algorithm is well-known to yield optimal convergence whenever all high frequency error components are associated with large relative eigenvalues. This ensures that smoothers like Gauss-Seidel and Jacobi will significantly dampen high frequency error components, and thus, generate smooth error. It has often been noted that this is true for matrices generated from standard discretizations of most elliptic equations. In this paper, we address a system of equations that is generated from a perturbation of the non-elliptic operator  $\mathbf{I} - \mathbf{grad\,div}$  by a negative  $\varepsilon \mathbf{\Delta}$ . For  $\varepsilon$  near to one, this operator is elliptic, but as  $\varepsilon$  approaches zero, the operator behaves like the non-elliptic operator  $\mathbf{I} - \mathbf{grad\,div}$ . This non-elliptic operator has been studied in several papers, and subsequently, it is widely known that discretizing the problem with the proper finite element space allows one to define a robust geometric multigrid algorithm. Here we use this work to assist in understanding the perturbed problem. We will introduce a new finite element space to discretize the problem and a relaxation operator used in the context of this new space that guarantees that the smoother leaves no high frequency error components behind. This is theoretically expressed in a theorem that proves that the multigrid algorithm converges independent of the mesh size and the parameter  $\varepsilon$ . Copyright © 2000 John Wiley & Sons, Ltd.

KEY WORDS: finite elements; divergence-free; multigrid methods

## 1. INTRODUCTION

A study of multigrid approaches for solving matrix equations generated from the 3D linear Boltzmann equation when formulated using a scaled least-squares functional (see [2], [11]) has revealed the need to understand finite element discretization and multigrid solution methods for a particular second-order partial differential equation. For a bounded, connected domain  $\Omega \subset \mathbf{R}^3$  with Lipschitz boundary  $\Gamma$ , this differential equation is

$$\begin{aligned} \mathbf{u} - \varepsilon \mathbf{\Delta} \mathbf{u} - \nabla \nabla \cdot \mathbf{u} &= \mathbf{f} \text{ in } \Omega \\ \mathbf{u} &= \mathbf{g} \text{ on } \Gamma, \end{aligned} \tag{1}$$

---

\*Correspondence to: austint@t7.lanl.gov

<sup>†</sup>This work is also referred to as LAUR-02 7191 and was sponsored by the National Science Foundation under grant number DMS-8704169 and Department of Energy, Applied Math Program Grant DE-FG03-94ER25217.

where  $\varepsilon \in (0, 1]$  and  $\mathbf{\Delta} := \text{diag}(\Delta)$ . Although the system arises in 3D, the simpler case of a 2D bounded polygonal domain is studied here. We will present 3D results in a future paper in the context of a scaled least-squares formulation of the 3D linear Boltzmann equation. Also, see [2] for 3D results.

A 2D system of this form was recently addressed by Mardal et al. in the context of Darcy-Stokes flow (see [12]), where a nonconforming finite element space on triangular elements for discretizing the variational formulation of (1) is introduced. On each triangular element, this FE space has nine degrees of freedom given by two normal components and a tangential component on each triangle edge. In that paper, the authors do not provide a robust solution method for solving the discrete system of equations. Here, we present a conforming tensor-product finite element space on rectangles for discretizing the variational formulation of (1), and describe a robust multigrid method that is easily constructed in the context of this conforming finite element space. We also include numerics that strongly suggest that the multigrid algorithm converges with a factor bounded away from unity and independent of both mesh size and parameter  $\varepsilon$ . Theoretical results will bolster this claim by illustrating that convergence of the multigrid algorithm, in the case where  $\varepsilon = 0$ , is independent of mesh size. Boundary conditions will be different, as in (2) below, for this value of  $\varepsilon$ . For reference purposes, we express the reduced system as follows:

$$\begin{aligned} \mathbf{u} - \nabla \nabla \cdot \mathbf{u} &= \mathbf{f} \text{ in } \Omega \\ \mathbf{n} \cdot \mathbf{u} &= g \text{ on } \Gamma, \end{aligned} \tag{2}$$

where  $\mathbf{n}$  is the unit vector that is outward normal to  $\Gamma$ . We note that the lowest order Raviart-Thomas finite element space on triangles, called  $\mathbf{RT}_0$  here (cf. [7], [9]), is a common choice for discretizing (2).

In [1], Arnold et al. presented a robust multigrid strategy for preconditioning the discrete system of equations that arises from discretizing the variational formulation of (2) with  $\mathbf{RT}_0$  elements. The main factor behind the robustness of their multigrid method is the utilization of an appropriate relaxation operator that guarantees a smooth error after relaxation. It is well known that standard relaxation schemes (e.g Gauss-Seidel, Jacobi) would fail in this case. While they substantially dampen error components associated with large eigenvalues, they do not dampen error components associated with small eigenvalues. Hence, those components that are div-free, or nearly div-free, are effectively not attenuated. These components can also be regarded as the near null space components of the operator. Since these components can be arbitrarily oscillatory, geometric smoothing will not occur for the error. This is equivalent to  $\mathbf{I} - \mathbf{grad} \text{ div}$  not being an elliptic operator. Vassilewski and Wang in [13] were the first to study multilevel solution approaches for solving the discrete system of equations derived from (2). Their approach constructs the local div-free functions and their orthogonal complements in the finite element space. We are more interested in the work of Arnold et al. because they do not use explicit construction. Instead, they simply use a group smoothing approach on appropriately chosen local subdomains. What binds the theory behind these two approaches, though, is their dependence on the ability to express the  $\mathbf{RT}_0$  finite element space in a discrete Helmholtz decomposition.

We should also note that work has been undertaken in 3D on this problem. Hiptmair and Hoppe in [10] describe a geometric multigrid approach that is similar to both 2D approaches discussed above. Their approach uses an idea that is essentially distributed relaxation, which was mentioned in early work of Brandt [5], to handle the troublesome div-free components.

The main idea is to take on the div-free relaxation in a higher-order space, which amounts to performing a Gauss-Seidel relaxation on Poisson's equation. This approach directly translates to our problem, but requires us to use multigrid methods for biharmonic equations. We will not discuss this idea here as the Arnold approach is more suitable as it avoids going to a fourth-order problem. Nonetheless, see [10] for this work on  $\mathbf{I} - \mathbf{grad} \operatorname{div}$  in 3D.

In the rest of the paper, we proceed as follows. In the next section, notation is introduced and the weak formulation corresponding to (1) is defined. Section 3 contains the description of the 2D cubic-quadratic conforming finite element space. The multigrid algorithm for solving the discrete problem is laid out in section 4. In section 5, we provide numerical results to confirm that the multigrid algorithm has optimal convergence. The numerical results suggest that convergence improves as  $\varepsilon > 0$  increases. In section 6, we will prove that for  $\varepsilon = 0$ , our multigrid algorithm will converge with rates independent of the mesh. We end with final remarks in section 7.

## 2. PRELIMINARIES

For  $\Omega \subset \mathbb{R}^2$ , denote by  $\mathcal{C}^k(\Omega)$  the class of continuous functions on  $\Omega$  with  $k$  continuous derivatives, and by  $\mathcal{C}^\infty(\Omega)$  the class of infinitely differentiable functions on  $\Omega$ . For the classical Hilbert spaces,  $\mathbf{H}^m(\Omega)$ , the standard conventions for representing norms are used:

$$\|v\|_{m,\Omega}^2 := \sum_{|\alpha| \leq m} \int_{\Omega} |\partial^\alpha v|^2 \, dx \, dy \quad \text{and} \quad |v|_{m,\Omega}^2 := \sum_{|\alpha|=m} \int_{\Omega} |\partial^\alpha v|^2 \, dx \, dy.$$

Also,  $L^2(\Omega) = \mathbf{H}^0(\Omega)$ ,  $\mathcal{C}_0^\infty(\Omega)$  refers to the subset of  $\mathcal{C}^\infty(\Omega)$  with compact support, and  $\mathbf{H}_0^m(\Omega)$  represents the closure of  $\mathcal{C}_0^\infty(\Omega)$  in the norm  $\|\cdot\|_{m,\Omega}$ . For the product space  $\mathbf{H}^m(\Omega)^2$  the alternate, and simpler, bold notation of  $\mathbf{H}^m(\Omega)$  will be used. Let  $\|\cdot\|_{m,\Omega}$  and  $|\cdot|_{m,\Omega}$  also represent norms and semi-norms for product spaces. The use of the scalar or the product definition will be clear from the context.

For  $\mathbf{u} = (u_1, u_2)^t$  and  $\mathbf{v} = (v_1, v_2)^t$ , the  $L^2$  inner product is

$$\langle \mathbf{u}, \mathbf{v} \rangle_{0,\Omega} := \langle u_1, v_1 \rangle_{0,\Omega} + \langle u_2, v_2 \rangle_{0,\Omega},$$

which yields the norm  $\|\mathbf{v}\|_{0,\Omega}^2 := \langle \mathbf{v}, \mathbf{v} \rangle$ . Similar norms and inner products exist for the other  $\mathbf{H}^m(\Omega)$  spaces. For  $\nabla \mathbf{u} = (\nabla u_1, \nabla u_2)^t$ , we also define

$$\langle \nabla \mathbf{u}, \nabla \mathbf{v} \rangle_{0,\Omega} := \langle \nabla u_1, \nabla v_1 \rangle_{0,\Omega} + \langle \nabla u_2, \nabla v_2 \rangle_{0,\Omega},$$

which yields the semi-norm  $|\mathbf{v}|_{1,\Omega}^2 := \|\nabla \mathbf{v}\|_{0,\Omega}^2$ . In the remainder, whenever the meaning is clear, the subscript  $\Omega$  will be omitted from inner products and norms as well as the subscript 0 from the  $L^2$  inner product and norm.

Next, consider the Hilbert space

$$\mathbf{H}(\operatorname{div}) := \{ \mathbf{v} \in L^2(\Omega)^2 : \operatorname{div} \mathbf{v} \in L^2(\Omega) \},$$

where  $\operatorname{div} \mathbf{v} = \partial_x v_1 + \partial_y v_2$ . The inner product for  $\mathbf{H}(\operatorname{div})$  is given by

$$\Lambda(\mathbf{u}, \mathbf{v}) := \langle \mathbf{u}, \mathbf{v} \rangle + \langle \operatorname{div} \mathbf{u}, \operatorname{div} \mathbf{v} \rangle \tag{3}$$

and its corresponding norm is written as  $\|\mathbf{u}\|_\Lambda := \sqrt{\Lambda(\mathbf{u}, \mathbf{u})}$ . We also must consider a subspace,  $\mathbf{H}_0(\text{div})$ , given by

$$\mathbf{H}_0(\text{div}) = \{\mathbf{v} \in \mathbf{H}(\text{div}) : \mathbf{v} \cdot \mathbf{n} = 0 \text{ on } \Gamma\},$$

where  $\Gamma := \partial\Omega$  and  $\mathbf{n}$  is as defined in the introduction. Additionally, we will refer to the *grad-perp* operator, which is given by

$$\nabla^\perp = (-\partial_y, \partial_x)^t.$$

Next, the addition of an  $\varepsilon$ -sized  $\mathbf{H}^1$  term to  $\|\mathbf{v}\|_\Lambda^2$  leads to the definition

$$\|\mathbf{v}\|_\varepsilon^2 := \|\mathbf{v}\|^2 + \|\text{div } \mathbf{v}\|^2 + \varepsilon \|\nabla \mathbf{v}\|^2. \quad (4)$$

With a closure taken with respect to  $\|\cdot\|_\varepsilon$  we get the spaces

$$\mathbf{V} := \overline{(\mathcal{C}^\infty(\Omega))^2} \quad \text{and} \quad \mathbf{V}_0 := \overline{(\mathcal{C}_0^\infty(\Omega))^2}.$$

Note that  $\mathbf{V}(\Omega)$  and  $\mathbf{H}^1(\Omega)$  are algebraically and topologically equivalent for  $\varepsilon > 0$  and only differ in their respective metrics. This equivalency also holds for  $\mathbf{V}_0(\Omega)$  and  $\mathbf{H}_0^1(\Omega)$ .

We now define the weak formulation of (1). For simplicity, we concentrate on the case of homogeneous boundary data in (1). Hence, the weak formulation becomes: seek  $\mathbf{u} \in \mathbf{V}_0$  such that

$$\mathcal{A}_\varepsilon(\mathbf{u}, \mathbf{v}) = f(\mathbf{v}), \quad \forall \mathbf{v} \in \mathbf{V}_0, \quad (5)$$

where

$$\mathcal{A}_\varepsilon(\mathbf{u}, \mathbf{v}) := \langle \mathbf{u}, \mathbf{v} \rangle + \varepsilon \langle \nabla \mathbf{u}, \nabla \mathbf{v} \rangle + \langle \text{div } \mathbf{u}, \text{div } \mathbf{v} \rangle,$$

and  $f(\mathbf{v}) := \langle \mathbf{f}, \mathbf{v} \rangle$ . If  $\mathbf{f} \in \mathbf{V}'_0$ , where  $\mathbf{V}'_0$  denotes the dual space to  $\mathbf{V}_0$ , then a unique solution to (5) exists in the Hilbert space  $\mathbf{V}_0$  as a result of the Riesz Representation Theorem [6].

To turn (5) into a discrete problem, we use finite elements. Although carefully constructed nonconforming finite elements leads to reasonable convergence (see [12]), a robust multilevel algorithm for the resulting linear system is not obvious. Here, we concentrate on conforming approaches. The discrete problem then reads: seek  $\mathbf{u}^h \in \mathbf{V}_0^h$  such that

$$\mathcal{A}_\varepsilon(\mathbf{u}^h, \mathbf{v}^h) = f(\mathbf{v}^h), \quad \forall \mathbf{v}^h \in \mathbf{V}_0^h, \quad (6)$$

where  $\mathbf{V}_0^h \subset \mathbf{H}_0^1(\Omega)$ . As a result the solution  $\mathbf{u}^h$  is the element of  $\mathbf{V}_0^h$  that minimizes the error in the  $\|\cdot\|_\varepsilon$  norm. That is, if  $\mathbf{u}$  and  $\mathbf{u}^h$  are solutions of the variational problem (5) in  $\mathbf{V}_0$  and  $\mathbf{V}_0^h$ , respectively, then

$$\|\mathbf{u} - \mathbf{u}^h\|_\varepsilon = \inf_{\mathbf{v}^h \in \mathbf{V}_0^h} \|\mathbf{u} - \mathbf{v}^h\|_\varepsilon. \quad (7)$$

Before proceeding to the next section, where we present the FE space used in (6), we highlight the two main principles on which the FE space is based. The first principle is that the FE space needs to be continuous in order to be conforming in  $\mathbf{H}^1$ . The second principle is that the FE space must facilitate the elimination of div-free error components in a relaxation scheme. This principle does not typically hold for standard FE spaces. It does, however, hold for the **RT** finite elements often used to discretize (2) (cf. [1, 13]). However, the **RT** spaces consist of discontinuous functions. Instead, we define a new, higher-order conforming FE space that is based on the **RT** space. To this end, consider the following definition of the lowest order **RT** space on rectangles:

$$\mathbf{RT}_{[0]} := \left\{ \mathbf{v} \in \mathbf{H}(\text{div}; \Omega) : \mathbf{v}|_T = \begin{pmatrix} a_1 + b_1 x \\ a_2 + b_2 y \end{pmatrix} \right\}, \quad (8)$$

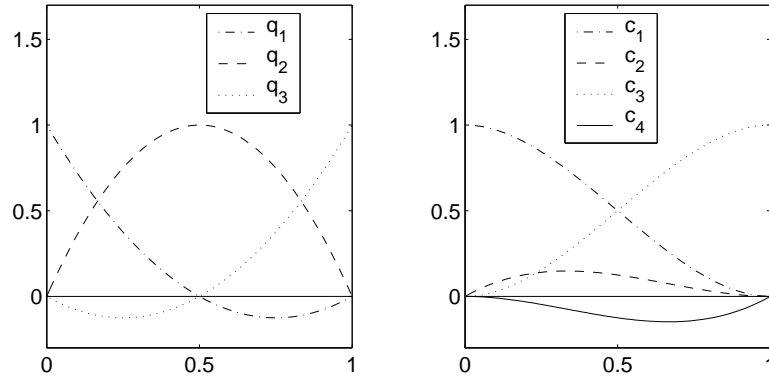


Figure 1. Shape functions for Lagrangian quadratics and Hermite cubics

where  $\Omega$  is partitioned into 2D rectangular elements  $T$ . This tensor-product FE space admits a basis for the div-free subspace with local support. This allows global div-free error components, which are also the near null space components, to be accurately represented through a basis with local support. Consequently, there exists an efficient smoother for global oscillatory div-free error. Motivated by common 1D finite element spaces, we present a space in the following section that has the same features as (8), except with more continuity. In the remainder, this space without boundary restrictions will be referred to as either  $\mathbf{MT}$  or  $\mathbf{MT}^h$ .

### 3. $\mathbf{RT}$ -LIKE CONTINUOUS FINITE ELEMENTS

In this section, we introduce our new finite element space, state and prove the existence of a discrete Helmholtz decomposition, and establish error bounds.

#### 3.1. Definition of elements

Consider the rectangular domain  $\Omega = I_x \times I_y$  for  $I_x = [a_x, b_x]$  and  $I_y = [a_y, b_y]$  given that  $a_x < b_x$  and  $a_y < b_y$ . Next, consider non-uniform partitions,  $I_{h_x}$  and  $I_{h_y}$ , represented by the sets of grid points:

$$a_x = x_0 < x_1 < \dots < x_{n-1} < x_n = b_x$$

and

$$a_y = y_0 < y_1 < \dots < y_{m-1} < y_m = b_y.$$

Let  $h_x = \max_{i=1,n} \{x_i - x_{i-1}\}$  and  $h_y = \max_{j=1,m} \{y_j - y_{j-1}\}$  and then denote the collection of non-uniform rectangular elements by  $\Omega^h = I_{h_x} \times I_{h_y}$  where  $h = \max \{h_x, h_y\}$ . We use the notation  $T$  or  $T_k$  to represent an arbitrary rectangular element and we use  $\mathcal{T}_h = \{T_k\}_{k=1}^{N_h}$  to denote the collection of all elements. Next, the FE space is constructed by separately defining the component spaces, i.e.,  $\mathbf{MT}^h := (M_{1h}, M_{2h})^t$ . Additional notation is needed to define this construction.

Let  $P_\ell(I)$  consist of all polynomials up to degree  $\ell$  on an arbitrary interval  $I$  and let

$$\mathcal{C}^{(m,n)}(\Omega) := \{f(x, y) \in \mathcal{C}(\Omega) : \partial_x^m f \in \mathcal{C}(\Omega) \text{ and } \partial_y^n f \in \mathcal{C}(\Omega)\}$$

and

$$\mathcal{C}^k(\Omega) := \{f(x, y) \in \mathcal{C}(\Omega) : \partial_x^{k_1} \partial_y^{k_2} f \in \mathcal{C}(\Omega) \text{ for } k_1 + k_2 \leq k\}.$$

Also, let  $I_{x,i} = [x_{i-1}, x_i]$  and  $I_{y,j} = [y_{j-1}, y_j]$  so that  $T_k = I_{x,i} \times I_{y,j}$  is an arbitrary rectangular element of  $\mathcal{T}_h$ . Now we define

$$\mathbf{M}_{1h} := \left\{ v^h : v^h \in \mathcal{C}^{(1,0)} \text{ and } v^h|_T \in P_3(I_{x,i}) \otimes P_2(I_{y,j}), \forall T \in \mathcal{T}_h \right\} \quad (9)$$

and

$$\mathbf{M}_{2h} := \left\{ v^h : v^h \in \mathcal{C}^{(0,1)} \text{ and } v^h|_T \in P_2(I_{x,i}) \otimes P_3(I_{y,j}), \forall T \in \mathcal{T}_h \right\}. \quad (10)$$

Finally,

$$\mathbf{MT}^h := \left\{ \begin{pmatrix} u_1 \\ u_2 \end{pmatrix} : \begin{array}{l} u_1 \in \mathbf{M}_{1h} \\ u_2 \in \mathbf{M}_{2h} \end{array} \right\}. \quad (11)$$

Next, we explain the nodal and edge degrees of freedom found in  $\mathbf{MT}^h$ .

Consider the 1D Lagrangian quadratic shape functions and the 1D Hermite cubic shape functions in Figure 1. On reference element  $T = [0, 1]^2$ , we define the following twelve 2D shape functions,

$$\phi_l(x, y) = c_{2i-1}(x)q_j(y) \quad \text{and} \quad \alpha_l(x, y) = c_{2i}(x)q_j(y),$$

where  $l = 3(i-1) + j$  for  $i = 1, 2$  and  $j = 1, 2, 3$ . Next, we place nodes on corners and edges of  $T$  as in Figure 2, and attach two degrees of freedom to each node. This allows the definition of the local interpolant

$$\Pi_{1h,T} v = \sum_{l=1}^6 N_l(v) \phi_l(x, y) + O_l(v) \alpha_l(x, y). \quad (12)$$

where

$$N_l(v) = v(\mathbf{x}_l) \quad \text{and} \quad O_l(v) = (\partial_x v)(\mathbf{x}_l).$$

These linear functions,  $N_l(v)$  and  $O_l(v)$ , have the properties

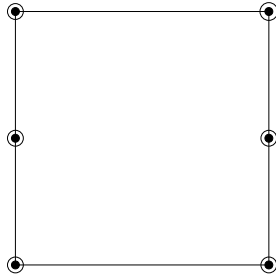
$$N_l(\phi_r) = \begin{cases} 1 & \text{if } r = l \\ 0 & \text{if } r \neq l \end{cases} \quad \text{and} \quad O_l(\alpha_r) = \begin{cases} 1 & \text{if } r = l \\ 0 & \text{if } r \neq l \end{cases}$$

and

$$N_l(\alpha_r) = 0 \quad \text{and} \quad O_l(\phi_r) = 0 \quad \forall r.$$

The interpolant in (12) is only defined on the reference element. We get a local interpolant for an arbitrary rectangular element,  $T_k$ , from the interpolant on the reference element in the usual way.

The shape functions and nodal variables for the second space,  $\mathbf{M}_{2h}$ , are obtained by reversing the roles of  $x$  and  $y$  in the definition of  $\mathbf{M}_{1h}$ . Therefore, degrees of freedom for  $\mathbf{M}_{2h}$  are defined on  $T$  by rotating the reference element in Figure 2 by 90 degrees. (Nodes sit on lower and upper edges.) Shape functions and nodal variables for  $\mathbf{M}_{2h}$  are defined in the same way as for  $\mathbf{M}_{1h}$ . We leave the details of these constructions to the reader, but we note that a similar local interpolant like that in (12) is obtained for  $\mathbf{M}_{2h}$ .

Figure 2. 2D Nodal Variables for  $v_1$  on a reference element  $T \in \mathcal{T}_h$ 

We finish with describing the construction of  $\mathbf{MT}^h$  by making two last comments. The first is that each space has a basis with local support. The second is that each local interpolant,  $\Pi_{ih,T}$ , leads to a global interpolant,  $\Pi_{ih}$ , and subsequently a global interpolant

$$\Pi_h := (\Pi_{1h}, \Pi_{2h})^t \quad (13)$$

for  $\mathbf{MT}^h$ . The exact nature of  $\Pi_{ih}$  for  $i = 1, 2$  is obtained from the respective local interpolant in the usual way. Error estimates will be presented in Section 3.3 for  $\Pi_h$ . Notation that we will use in the future to account for different boundary data is  $\mathbf{MT}_0^h := \mathbf{MT}^h \cap \mathbf{H}_0(\text{div})$  and  $\mathbf{MT}_{00}^h := \mathbf{MT}^h \cap \mathbf{H}_0^1(\Omega)$ .

*REMARK: While the above definition of  $\mathbf{MT}^h$  can be reasonably extended to general shaped domains, e. g. requiring isoparametric quadrilateral elements, the feature described in the next section, the discrete Helmholtz decomposition, only exists when we have a tensor product grid on a domain that is a union of overlapping rectangles.*

### 3.2. Discrete Helmholtz Decomposition

Two additional spaces are now introduced so that we can describe the div-free subspace of  $\mathbf{MT}^h$  and then a discrete Helmholtz decomposition for  $\mathbf{MT}^h$ . Later we discuss how the following propositions are affected by restricting to subspaces  $\mathbf{MT}_0^h$  and  $\mathbf{MT}_{00}^h$ . Hence, for the same mesh,  $\Omega^h$ , and elements,  $\mathcal{T}_h$ , as in the previous section, define the bi-Hermite cubic space

$$\mathbf{W}^h = \{w^h : w^h \in \mathcal{C}^1(\Omega) \text{ and } w^h|_T \in P_3(I_{x,i}) \otimes P_3(I_{y,j}), \forall T \in \mathcal{T}_h\}. \quad (14)$$

As is illustrated in the next proposition, the div-free subspace of  $\mathbf{MT}^h$  can be obtained from  $\mathbf{W}^h$  via *grad-perp* applied to  $\mathbf{W}^h$ . We shall denote this div-free subspace by  $\mathbf{DF}^h$ . The next proposition formalizes this relationship between  $\mathbf{W}^h$  and  $\mathbf{DF}^h$  for the case of no boundary conditions.

**Lemma 3.1.** *Assume that  $\Omega$  is a domain that is the union of overlapping rectangles. Next, let  $\mathcal{T}_h$  be the collection of rectangular elements obtained from a tensor product grid on  $\Omega$  such that  $\bar{\Omega} = \cup_{T \in \mathcal{T}_h} T$ . Then  $\mathbf{DF}^h = \nabla^\perp \mathbf{W}^h$ .*

*Proof.*

To prove this lemma, we show that the equality holds for the domain  $[0, 1]^2$ . From this result, one can easily show that it holds for an arbitrary rectangular element, and hence, for a domain that can be expressed as the union of rectangular elements.

Proving the equality for  $\Omega = [0, 1]^2$  requires that we show inclusion in both directions. The proof of  $\nabla^\perp W^h \subset \mathbf{DF}^h$  is simple and is left for the reader to verify. We do note that for  $w \in W^h$ ,  $\nabla^\perp w \in \mathbf{MT}^h$  only holds on a tensor product grid. (See Remark above.)

To prove that  $\mathbf{DF}^h \subset \nabla^\perp W^h$ , we must show that, for any  $\boldsymbol{\delta} = (\delta_1, \delta_2)^t \in \mathbf{DF}^h$ , there exists a  $w^* \in W^h$  such that  $\boldsymbol{\delta} = \nabla^\perp w^*$ . This is accomplished by construction. Before  $w^*$  is defined, a useful alternate representation of  $\delta_1$  is introduced. The expression is based on the fact that, by definition,

$$\partial_x \delta_1 = -\partial_y \delta_2.$$

By integrating the above equation over  $[0, x]$  we get

$$\delta_1(x, y) = -\partial_y \int_0^x \delta_2(\xi, y) \, d\xi + \delta_1(0, y). \quad (15)$$

Subsequently, set

$$w(x, y) = w_1(x, y) + w_2(x, y) := -\int_0^x \delta_2(\xi, y) \, d\xi + \int_0^y \delta_1(0, \eta) \, d\eta. \quad (16)$$

We must show that

$$\delta_1(x, y) = \partial_y w(x, y) \quad \text{and} \quad \delta_2(x, y) = -\partial_x w(x, y) \quad (17)$$

and, in addition, that  $w(x, y) \in W^h$ .

For the first equality of (17), the definition of  $w$  in (16) yields

$$\delta_1(x, y) = -\partial_y \int_0^x \delta_2(\xi, y) \, d\xi + \delta_1(0, y). \quad (18)$$

As established in (15), the right hand side of (18) is simply an alternative expression for  $\delta_1(x, y)$ . For the second equality of (17), we simply note that by definition of  $w$ , and the fundamental theorem of calculus,  $\delta_2 = \partial_x w$ . Finally, we need to confirm that  $w \in W^h$ .

Recall the meaning of  $w \in \mathcal{C}^{1,1}(\Omega)$ :  $w$  is a  $\mathcal{C}^1$  function in  $x$  and in  $y$ . This can be established by looking at each summand of (16). The first summand,  $w_1$ , is  $\mathcal{C}^1$  in  $y$  because  $\delta_2(x, y)$  has the required continuity and the integration does not affect this continuity. Next, it is  $\mathcal{C}^1$  in  $x$  because  $\delta_2(x, y)$  is  $\mathcal{C}^0$  in  $x$  (and since the  $x$ -derivative of  $w$  is  $\delta_2$ ). A similar line of reasoning implies  $w_2$  is also  $\mathcal{C}^1$ , and therefore,

$$w(x, y) \in \mathcal{C}^1(\Omega). \quad (19)$$

This proves that there exists a  $w^* \in W^h$  such that  $\boldsymbol{\delta} = \nabla^\perp w^*$ .  $\square$

We proved Lemma 3.1 for the case that no boundary conditions are enforced on the FE space. If boundary conditions are enforced, as in  $\mathbf{MT}_0^h$  or  $\mathbf{MT}_{00}^h$ , we do need a different pre-image space for the *grad-perp* operator to generate  $\mathbf{DF}_0^h$  and  $\mathbf{DF}_{00}^h$ . The two appropriate subspaces of  $W^h$  are given by

$$W_0^h = \{w \in W^h : w = 0 \text{ on } \Gamma\}$$



and

$$W_{00}^h = \{w \in W^h : w = 0 \text{ and } \mathbf{n} \cdot \nabla w = 0 \text{ on } \Gamma\}.$$

With these definitions, we state an additional lemma that defines  $\mathbf{DF}_0^h$  and  $\mathbf{DF}_{00}^h$ .

**Lemma 3.2.** *Under the same conditions as Lemma 3.1 we have that  $\mathbf{DF}_0^h = \nabla^\perp W_0^h$  and that  $\mathbf{DF}_{00}^h = \nabla^\perp W_{00}^h$ .*

*Proof*

We do not prove this lemma with the same rigor as with the previous one. Instead, we just provide the reader with the definition of  $w$  on  $[0, 1]^2$  and leave out the remaining details. On that note, we have

$$w(x, y) = \int_0^x \delta_2(\xi, y) \, d\xi \tag{20}$$

for both cases in question. The boundary conditions on  $\delta$  plus (15) yields the boundary conditions on  $w$ .  $\square$

To define a discrete Helmholtz decomposition for the subspaces of  $\mathbf{MT}^h$ , we investigate the structure of the  $L^2$ -orthogonal complement of the div-free components. To that end, a third FE space is introduced. For the same mesh,  $\Omega^h$ , and elements,  $\mathcal{T}_h$ , consider the bi-Lagrangian quadratic space

$$S^h := \{s^h : s^h \in C^0(\Omega) \text{ and } s^h|_T \in P_2(I_x) \otimes P_2(I_y), \forall T \in \mathcal{T}_h\} \tag{21}$$

and also let  $\hat{S}^h := S^h/\mathbf{R}$ . Through  $\hat{S}^h$  we define the discrete gradient operator with regards to  $\mathbf{MT}_0^h$ .

**Definition 3.3.** *For  $s^h \in \hat{S}^h$ , define  $\nabla_h s^h \in \mathbf{MT}_0^h$  by*

$$\langle \nabla_h s^h, \mathbf{v}^h \rangle = -\langle s^h, \operatorname{div} \mathbf{v}^h \rangle, \quad \forall \mathbf{v}^h \in \mathbf{MT}_0^h.$$

The element  $\nabla_h s^h$  is a uniquely determined because the functional  $\langle s^h, \operatorname{div} \mathbf{v}^h \rangle$  is well defined and continuous, which allows us to invoke the Riesz Representation Theorem [6]. A definition of  $\nabla_h$  also exists with regards to  $\mathbf{MT}_{00}^h$  by replacing  $\mathbf{MT}_0^h$  with  $\mathbf{MT}_{00}^h$  and then replacing  $\hat{S}^h$  with  $S_0^h = S^h \cap H_0^1$ .

Definition 3.3 implies that, in both  $\mathbf{MT}_0^h$  and  $\mathbf{MT}_{00}^h$ , discrete gradients are orthogonal to div-free elements with respect to the  $L^2$  inner product, and additionally, with respect to the inner product  $\Lambda(\cdot, \cdot)$  seen in (3). This leads to the discrete Helmholtz decomposition, which is the next theorem. The proof of this theorem mimics the proof used in establishing a similar result for the  $\mathbf{RT}$  spaces (e.g., [3]). We prove this for the more general case of  $\mathbf{MT}_0^h$ . A similar proof holds for  $\mathbf{MT}_{00}^h$ .

**Theorem 3.4.** *(Discrete Helmholtz Decomposition) Assume that  $\mathcal{T}_h$  is the collection of rectangular elements obtained from a tensor product grid as in Lemma 3.1 and that  $\bar{\Omega} = \cup_{T \in \mathcal{T}_h} T$ . Then  $\mathbf{MT}_0^h$  admits the following  $L^2$ -orthogonal decomposition:*

$$\mathbf{MT}_0^h = \nabla_h \hat{S}^h \oplus \nabla^\perp W_0^h. \tag{22}$$

*Proof*

The  $L^2$  orthogonality is proved first. Let  $s^h \in \hat{S}^h$  and  $w^h \in W_0^h$  such that  $\nabla_h s^h \in \nabla_h \hat{S}^h$  and  $\nabla^\perp w^h \in \nabla^\perp W_0^h$ . Then, by definition of  $\nabla_h$ ,

$$\langle \nabla_h s^h, \nabla^\perp w^h \rangle = \langle s^h, \nabla \cdot (\nabla^\perp w^h) \rangle = 0.$$

Thus,  $\nabla_h \hat{S}^h \perp_{L^2} \nabla^\perp W_0^h$ .

Now equality is proved by showing inclusion in both directions. We first note that  $\nabla_h \hat{S}^h \subset \mathbf{MT}_0^h$ , which is true by definition, and  $\nabla^\perp W_0^h \subset \mathbf{MT}_0^h$ , which is guaranteed by Lemma 3.2. Then,  $\nabla_h \hat{S}^h + \nabla^\perp W_0^h \subset \mathbf{MT}_0^h$ . To get inclusion in the other direction, let  $\mathbf{v}^h \in \mathbf{MT}_0^h$  and set  $\mathbf{g}^h$  to be the projection of  $\mathbf{v}^h$  onto  $\nabla_h \hat{S}^h$ , i.e.,

$$\langle \mathbf{v}^h - \mathbf{g}^h, \nabla_h s^h \rangle = 0, \quad \forall s^h \in \hat{S}^h.$$

Using Definition 3.3, we can say

$$\langle \nabla \cdot (\mathbf{v}^h - \mathbf{g}^h), s^h \rangle = 0, \quad \forall s^h \in \hat{S}^h.$$

Since  $\nabla \cdot (\mathbf{v}^h - \mathbf{g}^h) \in \hat{S}^h$  by definition, this implies that  $\nabla \cdot (\mathbf{v}^h - \mathbf{g}^h) = 0$ . As a result,  $\mathbf{v}^h - \mathbf{g}^h \in \nabla^\perp W_0^h$ . Since  $\mathbf{v}^h$  was arbitrarily chosen,

$$\mathbf{MT}_0^h \subset \nabla_h \hat{S}^h \oplus \nabla^\perp W_0^h,$$

which proves (22).  $\square$

According to Theorem 3.4, for any  $\mathbf{u} \in \mathbf{MT}_0^h$ , there exists a mapping  $\mathcal{G}_h : \mathbf{MT}_0^h \rightarrow \hat{S}^h$  and  $\mathcal{F}_h : \mathbf{MT}_0^h \rightarrow W_0^h$  such that

$$\mathbf{u} = \nabla_h(\mathcal{G}_h \mathbf{u}) + \nabla^\perp(\mathcal{F}_h \mathbf{u}). \quad (23)$$

Notice that the two components of this decomposition are not orthogonal with respect to the  $\mathcal{A}_\varepsilon(\cdot, \cdot)$  inner product for  $\varepsilon$  greater than zero. Also, if we consider the case  $\mathbf{MT}_{00}^h$ , then we obtain a similar decomposition in terms of  $W_{00}^h$  and  $S_0^h$ .

### 3.3. Error estimates

Let  $\Pi_h \mathbf{v} \in \mathbf{MT}^h$  be the interpolant of  $\mathbf{v}$  as in (13). Let  $c$  and  $C$  denote arbitrary constants, which may depend on certain domain properties but not on mesh sizes or the parameter  $\varepsilon$ . The following lemma states without proof a standard interpolation result for  $\Pi_h$ .

**Lemma 3.5.** *Assume that  $\mathcal{T}_h$  is a collection of rectangular elements and that  $\bar{\Omega} = \cup_{T \in \mathcal{T}_h} T$ . Set  $h = \max_{T \in \mathcal{T}_h} h_T$  and let  $\Pi_h$  be the interpolation operator of  $\mathbf{MT}^h$ . For  $\mathbf{v} \in \mathbf{H}^k(\Omega)$ ,  $2 \leq k \leq 3$ , we get the following bound:*

$$\|\mathbf{v} - \Pi_h \mathbf{v}\|_{m, \Omega} \leq Ch^{k-m} |\mathbf{v}|_{k, \Omega}, \quad (24)$$

where  $0 \leq m < k$ .

*Proof*

The proof uses standard techniques that are employed in proofs of similar claims for tensor product finite element spaces. See [3] or [6] for an outline of such a proof.  $\square$

A bound on the divergence of the interpolation error requires the inequality

$$\|\operatorname{div} \mathbf{v}\|_{0, \Omega} \leq \|\operatorname{div} \mathbf{v}\|_{0, \Omega} + \|\nabla \times \mathbf{v}\|_{0, \Omega} \leq \sqrt{2} |\mathbf{v}|_{1, \Omega}.$$

The error bound for the divergence, using this inequality, is

$$\|\operatorname{div}(\mathbf{v} - \Pi_h \mathbf{v})\|_{0,\Omega} \leq Ch^{k-1} |\mathbf{v}|_{k,\Omega}, \quad (25)$$

where  $2 \leq k \leq 3$  and  $\sqrt{2}$  has been absorbed into  $C$ .

In the remainder of this section, we consider (1) with homogeneous boundary conditions. Using (7), (24), and (25), convergence of the approximate solution in FE space  $\mathbf{MT}_{00}^h$  to the exact solution as  $h \rightarrow 0$  is established in terms of the  $\|\cdot\|_\varepsilon$  norm.

**Theorem 3.6.** *Assume that  $\mathcal{T}_h$  is a collection of rectangular elements and that  $\bar{\Omega} = \cup_{T \in \mathcal{T}_h} T$ . Then set  $h = \max_{T \in \mathcal{T}_h} h_T$ . Next, assume that solution  $\mathbf{u}$  of (5) is in  $\mathbf{H}^k(\Omega) \cap \mathbf{H}_0^1(\Omega)$  for  $k = 2, 3$ . If  $\mathbf{u}^h \in \mathbf{MT}_{00}^h$  is the solution of (6), we have that the error,  $\mathbf{e}^h := \mathbf{u} - \mathbf{u}^h$ , satisfies*

$$\|\mathbf{e}^h\|_{\varepsilon,\Omega} \leq Ch^{k-1} |\mathbf{u}|_{k,\Omega}. \quad (26)$$

*Proof*

The proof follows from (7), the observation that

$$\inf_{\mathbf{v}^h \in \mathbf{MT}_{00}^h} \|\mathbf{u} - \mathbf{v}^h\|_{\varepsilon,\Omega} \leq \|\mathbf{u} - \Pi_h \mathbf{u}\|_{\varepsilon,\Omega},$$

and the following estimates, using (24) and (25):

$$\begin{aligned} \|\mathbf{u} - \Pi_h \mathbf{u}\|_{\varepsilon,\Omega}^2 &= \|\mathbf{u} - \Pi_h \mathbf{u}\|_{0,\Omega}^2 + \varepsilon \|\mathbf{u} - \Pi_h \mathbf{u}\|_{1,\Omega}^2 + \|\operatorname{div}(\mathbf{u} - \Pi_h \mathbf{u})\|_{0,\Omega}^2 \\ &\leq C_1 h^{2k} |\mathbf{u}|_{k,\Omega}^2 + C_2 \varepsilon h^{2k-2} |\mathbf{u}|_{k,\Omega}^2 + C_3 h^{2k-2} |\mathbf{u}|_{k,\Omega}^2 \\ &\leq Ch^{2k-2} |\mathbf{u}|_{k,\Omega}^2. \end{aligned}$$

Taking the square root of both sides completes the proof.  $\square$

We should note that, numerically, we see a better order of convergence of the error for  $\varepsilon \approx 0$  than is implied by the theorem above. This is a result of our inability to derive a tighter bound on the divergence of the error than that which is seen in (25).

#### 4. MULTIGRID ALGORITHM

In this section, we introduce an effective multigrid algorithm that can be used to solve the discrete systems arising from (6) with  $\mathbf{V}_0^h = \mathbf{MT}_{00}^h$ . To this end, assume a coarse triangulation  $\mathcal{T}_0$  of  $\Omega$  and let  $\mathbf{MT}_0$  denote  $\mathbf{MT}_{00}^h$  restricted to this coarse mesh. By halving the spatial cells in each direction, we get a series of finer meshes and richer FE spaces. The sequence of successively finer spaces will be denoted by

$$\mathbf{MT}_0 \subset \mathbf{MT}_1 \subset \cdots \subset \mathbf{MT}_{J-1} \subset \mathbf{MT}_J. \quad (27)$$

All coarse grid problems are realized by simply restricting variational problem (6) to the coarser spaces. In this context, interpolation becomes simple injection and restriction is the transpose of interpolation (see [3]). In the remainder of this section, we describe an overlapping block Jacobi and an overlapping block Gauss-Seidel relaxation technique, which eliminates high frequency div-free error.

For  $j \in \{1, \dots, J\}$ , consider  $\mathbf{MT}_j$  defined on triangulation  $\mathcal{T}_j$ . Let  $\mathcal{N}_j$  correspond to vertices of the rectangular mesh. Let the set  $\mathcal{T}_{j,\nu}$  be the collection of elements with common vertex  $\nu$ ,

and  $\Omega_{j,\nu}$  be the interior of the subdomain formed by the union of these elements. Now, define  $\mathbf{MT}_{j,\nu}$  as

$$\mathbf{MT}_{j,\nu} := \left\{ \mathbf{v} \in \mathbf{MT}^h : \text{supp}\{\mathbf{v}\} \subseteq \bar{\Omega}_{j,\nu} \right\},$$

which is the subspace of  $\mathbf{MT}_j$  with support in  $\Omega_{j,\nu}$ .

Next, we rewrite discrete problem (6) as an operator equation. Define the discrete linear operator  $A_j^\varepsilon : \mathbf{MT}_j \rightarrow \mathbf{MT}_j$  by

$$\mathcal{A}_\varepsilon(\mathbf{u}, \mathbf{v}) = \langle A_j^\varepsilon \mathbf{u}, \mathbf{v} \rangle, \quad \forall \mathbf{u}, \mathbf{v} \in \mathbf{MT}_j. \quad (28)$$

Thus, the discrete problem on the finest grid is  $A_j^\varepsilon \mathbf{x}_J = \mathbf{b}_J$ , where  $\mathbf{b}_J \in \mathbf{MT}_J$  is defined by

$$\langle \mathbf{b}_J, \mathbf{v} \rangle = \langle \mathbf{f}, \mathbf{v} \rangle \quad \forall \mathbf{v} \in \mathbf{MT}_J.$$

Also, define projection operators  $\mathbf{P}_j : \mathbf{H}^1 \rightarrow \mathbf{MT}_j$  and  $Q_j : L^2 \rightarrow \mathbf{MT}_j$  according to

$$\mathcal{A}_\varepsilon(\mathbf{P}_j \mathbf{u}, \mathbf{v}) = \mathcal{A}_\varepsilon(\mathbf{u}, \mathbf{v}), \quad \forall \mathbf{v} \in \mathbf{MT}_j \quad (29)$$

and

$$\langle Q_j \mathbf{u}, \mathbf{v} \rangle = \langle \mathbf{u}, \mathbf{v} \rangle, \quad \forall \mathbf{v} \in \mathbf{MT}_j. \quad (30)$$

Locally we use projection operators corresponding to subdomains  $\Omega_{j,\nu}$  in the following way:  $\mathbf{P}_{j,\nu} : \mathbf{H}^1 \rightarrow \mathbf{MT}_{j,\nu}$  represents a local solve on  $\Omega_{j,\nu}$  according to

$$\mathcal{A}_\varepsilon(\mathbf{P}_{j,\nu} \mathbf{v}, \mathbf{w}) = \mathcal{A}_\varepsilon(\mathbf{v}, \mathbf{w}), \quad \forall \mathbf{w} \in \mathbf{MT}_{j,\nu}. \quad (31)$$

This is a local solve in the sense that  $\mathbf{P}_{j,\nu} \mathbf{v}$  is the local solution of a problem with right-hand side given by  $A_j^\varepsilon \mathbf{v}$ .

Before we define the additive smoother, we let  $\kappa$  be the maximum number of subdomains  $\Omega_{j,\nu}$  in which any point  $\mathbf{x} \in \Omega$  is included. The additive smoothing operator,  $R_j$ , is then

$$R_j := \eta \sum_{\nu \in \mathcal{N}_j} \mathbf{P}_{j,\nu} (A_j^\varepsilon)^{-1} \quad (32)$$

with scaling factor  $\eta$ , which must be less than  $1/\kappa$  to ensure that  $R_j$  is a contraction.

*Remark 1:* The additive smoothing operator  $R_j$  is  $L^2$ -symmetric and positive definite.

*Remark 2:* The definition of  $R_j$  yields

$$\eta \langle R_j^{-1} \mathbf{v}, \mathbf{v} \rangle = \inf_{\substack{\mathbf{v}_\nu \in \mathbf{MT}_{j,\nu} \\ \mathbf{v} = \sum_{\nu \in \mathcal{N}_j} \mathbf{v}_\nu}} \sum \mathcal{A}_\varepsilon(\mathbf{v}_\nu, \mathbf{v}_\nu),$$

which is proved in Appendix B of [1].

*Remark 3:* The work involved in performing the action of  $R_j$  involves inverting a  $12 \times 12$  symmetric positive definite matrix associated with each vertex  $\nu \in \mathcal{N}_j$  except at boundaries where the work is less.

A nonsymmetric multiplicative version of  $R_j$ , which we call  $\widehat{R}_j$  is defined algorithmically. To begin, assume an ordering of the vertices,  $\nu_l \in \mathcal{N}_j$ ,  $l = 1, \dots, N_j$ , and write  $\mathbf{P}_{j,\nu_l}$  as  $\mathbf{P}_{j,l}$

for now. Let the current iterate be given by  $\mathbf{x}^k$  with residual  $\mathbf{r}^k$ . Then the next iterate,  $\mathbf{x}^{k+1}$ , is the last step,  $\mathbf{x}_{N_j}^{k+1}$ , of the following sweep:

$$\mathbf{x}_{l+1}^{k+1} = \mathbf{x}_l^k + \mathbf{P}_{j,l} (\mathbf{A}_j^\varepsilon)^{-1} \mathbf{r}_l^k \quad \text{for } l = 1, 2, \dots, N_j, \quad (33)$$

where  $\mathbf{r}_l^k = (\mathbf{b} - \mathbf{A}_j^\varepsilon \mathbf{x}_l^k)$  and  $\mathbf{e}_l^k = (\mathbf{A}_j^\varepsilon)^{-1} \mathbf{r}_l^k$ . This algorithm defines the nonsymmetric multiplicative operator. A version that reverses the ordering of the smoothing of the sweep on the back end of the V-cycle yields a symmetric cycle.

To take into account the extra work required in performing the block relaxation, we introduce the Work Unit (WU), defined as the number of floating point operations to calculate the residual vector. One sweep of a pointwise smoother requires one WU. In comparison, due to the overlap of the subdomains  $\Omega_{j,\nu}$ , we need approximately 1.5 WUs to complete a sweep of the grid with the block relaxation.

With definitions of transfer operators and a relaxation approach, we can now use any of the multigrid cyclic strategies (e. g. W-cycles,  $V(\mu_1, \mu_2)$ -cycles, or FMG; see [8]). In our numerical results, we work solely with a standard V-cycle using  $m$  pre-smoothings of the nonsymmetric multiplicative relaxation operator and  $m$  post-smoothings of the adjoint of the nonsymmetric operator. Letting  $\mathcal{S}_j$  denote one of the relaxation operators,  $\mathbf{I}_{j-1}^j$  denote the interpolation operator, and  $\mathbf{I}_j^{j-1}$  denote the restriction operator, the standard  $V(m, m)$ -cycle is defined recursively:

Let  $\mathbf{B}_0 = (\mathbf{A}_0^\varepsilon)^{-1}$ . For  $j = 1, \dots, J$ , define  $\mathbf{B}_j \mathbf{f}$  for  $\mathbf{f} \in \mathbf{MT}_j$  as follows:

- (1) Set  $\mathbf{u}^0 = 0$  and  $\mathbf{r}^0 = 0$ .
- (2) (Pre-smoothing) Define  $\mathbf{u}^l$  for  $l = 1, \dots, m$  by

$$\mathbf{u}^l = \mathbf{u}^{l-1} + \mathcal{S}_j (\mathbf{f} - \mathbf{A}_j^\varepsilon \mathbf{u}^{l-1}).$$

- (3) Define  $\mathbf{w}^m = \mathbf{u}^m + \mathbf{I}_{j-1}^j \mathbf{q}$ , where

$$\mathbf{q} = \mathbf{B}_{j-1} \left[ \mathbf{I}_j^{j-1} (\mathbf{f} - \mathbf{A}_j^\varepsilon \mathbf{u}^m) \right].$$

- (4) (Post-Smoothing) Define  $\mathbf{w}^l$  for  $l = m+1, \dots, 2m$  by

$$\mathbf{w}^l = \mathbf{w}^{l-1} + \mathcal{S}_j^T (\mathbf{f} - \mathbf{A}_j^\varepsilon \mathbf{w}^{l-1}).$$

- (5) Set  $\mathbf{B}_j \mathbf{f} = \mathbf{w}^{2m}$ .

Then  $\mathbf{B}_j$  is a multilevel preconditioner for the discrete problem  $\mathbf{A}_j^\varepsilon \mathbf{x}_j = \mathbf{b}_j$ .

In the next section, we present numerical convergence results that were generated for a test problem posed on the unit square. Homogeneous data, i.e. zero right-hand side and zero Dirichlet boundary data, were used and the iterations began with a random initial guess for the interior unknowns.

## 5. NUMERICAL MULTILEVEL CONVERGENCE RESULTS

Asymptotic convergence rates are presented in Tables I and II for the  $V(1,1)$ -cycle with respect to two types of relaxation: either pointwise Gauss-Seidel relaxation or nonsymmetric

Table I. Asymptotic convergence results for V-cycle where  $\varepsilon = 10^{-1}$ 

$N_L$	$h_F$	$N_U$	$\sigma_B$	$\omega_B$	$\hat{\sigma}_B$	$\sigma_P$	$\omega_P$	$\hat{\sigma}_P$
2	1/4	112	0.209	4.0	0.676	0.652	2.67	0.852
3	1/8	480	0.212	4.0	0.679	0.715	2.67	0.882
4	1/16	1984	0.214	4.0	0.680	0.732	2.67	0.890
5	1/32	8064	0.215	4.0	0.681	0.736	2.67	0.892
6	1/64	32e3	0.216	4.0	0.682	0.737	2.67	0.892
7	1/128	13e4	0.216	4.0	0.682	0.738	2.67	0.892
8	1/256	52e4	0.216	4.0	0.682	0.739	2.67	0.892

Table II. Asymptotic convergence results for V-cycle where  $\varepsilon = 10^{-8}$ 

$N_L$	$h_F$	$N_U$	$\sigma_B$	$\omega_B$	$\hat{\sigma}_B$	$\sigma_P$	$\omega_P$	$\hat{\sigma}_P$
2	1/4	112	0.351	4.0	0.770	0.962	2.67	0.985
3	1/8	480	0.472	4.0	0.829	0.984	2.67	0.994
4	1/16	1984	0.502	4.0	0.842	0.993	2.67	0.997
5	1/32	8064	0.508	4.0	0.844	0.995	2.67	0.998
6	1/64	32e3	0.509	4.0	0.845	0.999	2.67	0.999
7	1/128	13e4	0.506	4.0	0.843	0.999	2.67	0.999
8	1/256	52e4	0.497	4.0	0.840	0.999	2.67	0.999

multiplicative block relaxation. Lexicographic ordering is used in both cases. Note that lexicographic ordering for block relaxation refers to how we sweep over the vertices, since each local group solve can be associated with a vertex in the same way that we defined  $\mathbf{MT}_{j,\nu}$  with reference to vertex  $\nu$  in section 4.

In both tables,  $N_L$  corresponds to the number of levels in the multigrid algorithm and then  $h_F = 1/2^{N_L}$  corresponds to the uniform fine grid mesh size. Note that a uniform grid is used in both directions. The third column shows the number of unknowns,  $N_U$ . The asymptotic convergence factor,  $\sigma_B$ , in column four provide an asymptotic measure of reduction in the energy norm of the error from a V-cycle using the nonsymmetric block smoother. In column five, we present  $\omega_B$ , the number of WUs to execute one complete V-cycle using the nonsymmetric block relaxation. We present the effective convergence factor,  $\hat{\sigma}_B := (\sigma_B)^{1/\omega_B}$  in column six. In the final three columns, we have the convergence factor, number of WUs, and the effective convergence factor,  $\hat{\sigma}_P := (\sigma_P)^{1/\omega_P}$ , for a V(1,1)-cycle using pointwise Gauss-Seidel.

In Figure 3, we consider a wide range of  $\varepsilon$  values for a fixed mesh size for the original  $\varepsilon$ -dependent problem, and for the  $\varepsilon$ -dependent problem with the identity term removed. Two observations can be made in response to these results. First, it appears that convergence is bounded as  $\varepsilon$  approaches zero. This, in addition to Tables I and II, indicate that our multigrid method is robust in  $\varepsilon$  and  $h$ . Second, the convergence results that we obtained when the identity term was removed imply that convergence of the original problem, as  $\varepsilon$  approaches zero, is mostly dependent on the resulting mass matrix term. Hence, in this limit, the best convergence that we can obtain is limited by what convergence we can get for the mass matrix

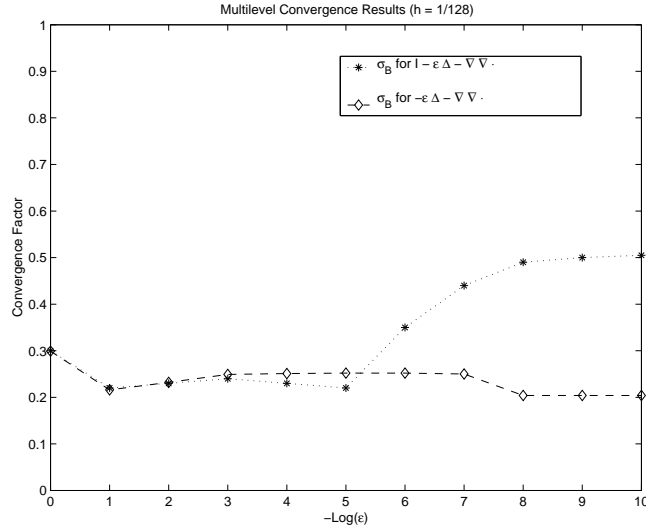


Figure 3. Multigrid Convergence Factor for fixed  $h$  and variable  $\varepsilon$  using Block Multiplicative Relaxation Operator

alone. As we can see, when the mass matrix is removed, convergence is greatly improved as  $\varepsilon$  goes to zero.

### 6. MULTILEVEL CONVERGENCE THEORY

In this section, we develop convergence theory for the multilevel method applied to the discrete equations that arise from a FE discretization of (2) with  $\mathbf{MT}_0^h$ . There are two reasons that we concentrate on (2) instead of the more general problem (1). First, a proof of the more general case where  $0 < \varepsilon \leq 1$  remains an open problem. Second, the numerical convergence results from Fig. 3, and Tables I and II, suggest that convergence appears to be bounded independent of  $h$ , but deteriorating with decreasing  $\varepsilon$ . Hence, if convergence is proved to be independent of  $h$  for  $\varepsilon = 0$ , that suggests the same should hold for  $\varepsilon > 0$ . For  $\varepsilon$  bounded away from zero, the results can be established using standard techniques (cf. [3] or [4]).

Since we are studying a slightly different system of equations when  $\varepsilon = 0$ , we make minor changes in notation for certain spaces and operators. To begin, any reference to  $\mathbf{MT}_j$  necessarily assumes that  $\mathbf{MT}_j \subset \mathbf{MT}_0^h$ . Next, the operators in (28) and (29) are redefined using the inner product  $\Lambda(\cdot, \cdot)$ . The discrete linear operator,  $\Lambda_j$ , is given by

$$\Lambda(\mathbf{u}, \mathbf{v}) = \langle \Lambda_j \mathbf{u}, \mathbf{v} \rangle, \quad \forall \mathbf{u}, \mathbf{v} \in \mathbf{MT}_j, \tag{34}$$

and thus, the discrete problem on the finest grid is  $\Lambda_J \mathbf{x}_J = \mathbf{b}_J$ . The projection operator,  $\mathbf{P}_j : \mathbf{H}(\text{div}) \rightarrow \mathbf{MT}_{j-1}$ , is given by

$$\Lambda(\mathbf{P}_j \mathbf{u}, \mathbf{v}) = \Lambda(\mathbf{u}, \mathbf{v}), \quad \forall \mathbf{v} \in \mathbf{MT}_j. \tag{35}$$

We also have a new definition of the operator  $\mathbf{P}_{j,\nu}$  that is described in (31). The operator  $\mathbf{P}_{j,\nu}$  was a local projection operator with respect to  $\mathcal{A}_\varepsilon(\cdot, \cdot)$ , but here it is a local projection

operator with respect to  $\Lambda(\cdot, \cdot)$ . Therefore, the additive smoothing operator (32) becomes

$$R_j := \eta \sum_{\nu \in \mathcal{N}_j} \mathbf{P}_{j,\nu} \Lambda_j^{-1}. \quad (36)$$

Given the interpolation and restrictions operators from Section 4, in addition to (36), we have the components needed to define the multilevel preconditioner,  $\mathbf{B}_j$ , for the equation  $\Lambda_j \mathbf{x}_J = \mathbf{b}_J$ .

In the remainder of this section, we prove convergence of the iteration using the preconditioned method that uses the additive smoothing operator (36) and then separately for the symmetric multiplicative counterpart to  $R_j$ . We make use of the following theorem, which can be found in Appendix B of [1]. Here,  $\mathcal{S}_j$  represents one of the aforementioned relaxation operators.

**Theorem 6.1.** *Suppose that, for each  $j = 1, \dots, J$ , relaxation operator  $\mathcal{S}_j$  satisfies*

$$\Lambda([\mathbf{I} - \mathcal{S}_j \Lambda_j] \mathbf{u}, \mathbf{u}) \geq 0, \quad \forall \mathbf{u} \in \mathbf{MT}_j, \quad (37)$$

and

$$(\mathcal{S}_j^{-1} [\mathbf{I} - \mathbf{P}_{j-1}] \mathbf{u}, [\mathbf{I} - \mathbf{P}_{j-1}] \mathbf{u}) \leq \alpha \Lambda([\mathbf{I} - \mathbf{P}_{j-1}] \mathbf{u}, [\mathbf{I} - \mathbf{P}_{j-1}] \mathbf{u}), \quad (38)$$

$$\forall \mathbf{u} \in \mathbf{MT}_j$$

where  $\alpha > 0$  is a constant. Then given  $m$  pre-smoothings and  $m$  post-smoothings of  $\mathcal{S}_j$  on level  $j$  for  $j = 1, \dots, J$ , multigrid operator  $\mathbf{B}_J$  satisfies

$$0 \leq \Lambda([\mathbf{I} - \mathbf{B}_J \Lambda_J] \mathbf{u}, \mathbf{u}) \leq \gamma \Lambda(\mathbf{u}, \mathbf{u}), \quad \forall \mathbf{u} \in \mathbf{MT}_J, \quad (39)$$

where  $\gamma = \frac{\alpha}{\alpha + m}$ .

*Proof*

See Appendix B of [1]. □

Since the result in Theorem 6.1 depends upon inequalities (37) and (38), the remainder of this section will be devoted to establishing these claims. We begin with (37) and (38) for the symmetric additive relaxation operator,  $R_j$ . Then these results are employed to confirm that both properties also hold for the symmetric multiplicative relaxation operator,  $\widehat{R}_j$ .

Before a proof of (37) or (38) can be established, we must establish two lemmas that are needed in proving the the second inequality. In both lemmas, we assume a coarse triangulation,  $\mathcal{T}_{j-1}$ , and a fine triangulation,  $\mathcal{T}_j$ , which is obtained from  $\mathcal{T}_{j-1}$  by halving the spatial cells in each direction. Each triangulation is associated with a mesh size,  $h_{j-1}$  and  $h_j$ , respectively. Also,  $\mathbf{MT}_{j-1}$  and  $\mathbf{MT}_j$  are the finite element spaces restricted to these meshes. Lastly, let  $\nabla_j$  denote the weak gradient operator relative to  $\mathbf{MT}_j$ .

**Lemma 6.2.** *Let  $\mathbf{u} \in \mathbf{MT}_j$  and let  $\mathbf{v} = [\mathbf{I} - \mathbf{P}_{j-1}] \mathbf{u} \in \mathbf{MT}_j$  have a discrete Helmholtz decomposition given by  $\mathbf{v} = \nabla_j s + \nabla^\perp w$ , where  $s \in \mathcal{S}_j/\mathbf{R}$  and  $w \in W_{0j} := W_j \cap \mathbf{H}_0^1$ . Then we have*

$$\|\nabla_j s\| \leq C h_{j-1} \|\mathbf{v}\|_{\mathbf{H}(\text{div})} \quad (40)$$

and

$$\|w\| \leq C h_{j-1} \|\mathbf{v}\|_{\mathbf{H}(\text{div})}, \quad (41)$$

where  $C$  represents an arbitrary positive constants that only depends on domain  $\Omega$ .

*Proof*



To prove (40), put  $\boldsymbol{\xi}_j = \Lambda_j^{-1}(\nabla_j s) \in \nabla_h S^h \subset \mathbf{MT}^h$ . Therefore,

$$\|\nabla_j s\|^2 = \langle \Lambda_j \nabla_j s, \Lambda_j^{-1}(\nabla_j s) \rangle = \Lambda(\nabla_j s, \boldsymbol{\xi}_j) \quad (42)$$

Furthermore,

$$\Lambda(\nabla_j s, \boldsymbol{\xi}_j) = \Lambda(\nabla_j s + \nabla^\perp w, \boldsymbol{\xi}_j) = \Lambda(\mathbf{u} - \mathbf{P}_{j-1} \mathbf{u}, \boldsymbol{\xi}_j). \quad (43)$$

Next, define  $\boldsymbol{\xi}_{j-1}$  as the solution of the equation

$$\Lambda(\boldsymbol{\xi}_{j-1} - \boldsymbol{\xi}_j, \mathbf{w}) = 0, \quad \forall \mathbf{w} \in \mathbf{MT}_{j-1}.$$

Approximation theory (cf. [3]) yields

$$\|\boldsymbol{\xi}_j - \boldsymbol{\xi}_{j-1}\|_{\mathbf{H}(\text{div})} \leq C h_{j-1} \|\Lambda_j \boldsymbol{\xi}_j\|, \quad (44)$$

for  $C$  an arbitrary constant. Using the right-hand side of (43), the bound in (44), and the definition of  $\boldsymbol{\xi}_j$ , we have

$$\begin{aligned} \Lambda(\mathbf{u} - \mathbf{P}_{j-1} \mathbf{u}, \boldsymbol{\xi}_j) &= \Lambda(\mathbf{u} - \mathbf{P}_{j-1} \mathbf{u}, \boldsymbol{\xi}_j - \boldsymbol{\xi}_{j-1}) \\ &\leq \|\mathbf{v}\|_{\mathbf{H}(\text{div})} \|\boldsymbol{\xi}_j - \boldsymbol{\xi}_{j-1}\|_{\mathbf{H}(\text{div})} \\ &\leq C h_{j-1} \|\mathbf{v}\|_{\mathbf{H}(\text{div})} \|\Lambda_j \boldsymbol{\xi}_j\| \\ &= C h_{j-1} \|\mathbf{v}\|_{\mathbf{H}(\text{div})} \|\nabla_j s\| \end{aligned}$$

Using (42) and (43) we then get

$$\|\nabla_j s\| \leq C h_{j-1} \|\mathbf{v}\|_{\mathbf{H}(\text{div})},$$

which establishes (40).

To prove (41), we first remark that  $w$  in (41) has the orthogonality property

$$(\nabla^\perp w, \nabla^\perp \hat{w}) = 0 \quad \forall \hat{w} \in W_{j-1}.$$

This implies a standard duality argument applies (cf. [3]), and consequently,

$$\|w\| \leq C h_{j-1} \|\nabla^\perp w\|.$$

The inequality (41) is automatic with the observation that

$$\|\nabla^\perp w\| = \|\nabla^\perp w\|_{\mathbf{H}(\text{div})} \leq \|\mathbf{v}\|_{\mathbf{H}(\text{div})}.$$

Therefore, we have proven (40) and (41).  $\square$

Next, we prove an additional bound on the  $\mathbf{H}^1$ -seminorm of the weak gradient component. The proof requires the assumption that the mesh size of consecutive levels, i.e.  $\mathbf{MT}_j$  and  $\mathbf{MT}_{j-1}$ , differ by a bounded factor, i.e.,  $h_{j-1} = ph_j$  where  $p$  typically equals two.

**Lemma 6.3.** *Let  $\mathbf{u} \in \mathbf{MT}_j$  and let  $\mathbf{v} = [\mathbf{I} - \mathbf{P}_{j-1}] \mathbf{u} \in \mathbf{MT}_j$  have a discrete Helmholtz decomposition given by  $\mathbf{v} = \nabla_j s + \nabla^\perp w$ , where  $s \in \mathbf{S}_j/\mathbf{R}$  and  $w \in W_{0j} := W_j \cap \mathbf{H}_0^1$ . Hence, we have*

$$|\nabla_j s|_1 \leq C \|\mathbf{v}\|_{\mathbf{H}(\text{div})} \quad (45)$$

for a positive constant  $C$  that only depends on domain  $\Omega$ .

*Proof*

First, an inverse estimate (cf. [3]) yields the inequality

$$|\nabla_j s|_1 \leq \frac{\bar{C}}{h_j} \|\nabla_h s\|$$

for some constant  $\bar{C}$ . Using (40) in Lemma 6.2, we have

$$|\nabla_j s|_1 \leq \bar{C} \frac{h_{j-1}}{h_j} \|\mathbf{v}\|_{\mathbf{H}(\text{div})}.$$

Then we can write

$$|\nabla_j s|_1 \leq \bar{C} p \|\mathbf{v}\|_{\mathbf{H}(\text{div})} \leq C \|\mathbf{v}\|_{\mathbf{H}(\text{div})},$$

where  $C$  depends only on domain  $\Omega$  for fixed  $p$ . □

### 6.1. Verification of (37) for Symmetric Additive Relaxation Operator

With the expansion  $R_j \Lambda_j = \eta \sum_{\nu \in \mathcal{N}_j} \mathbf{P}_{j,\nu}$ , we have, for  $\mathbf{u} \in \mathbf{MT}_j$ ,

$$\Lambda(R_j \Lambda_j \mathbf{u}, \mathbf{u}) = \eta \sum_{\nu \in \mathcal{N}_j} \Lambda(\mathbf{P}_{j,\nu} \mathbf{u}, \mathbf{u}),$$

which gives

$$\Lambda([\mathbf{I} - R_j \Lambda_j] \mathbf{u}, \mathbf{u}) = \Lambda(\mathbf{u}, \mathbf{u}) - \eta \sum_{\nu \in \mathcal{N}_j} \Lambda(\mathbf{P}_{j,\nu} \mathbf{u}, \mathbf{u}). \quad (46)$$

The Cauchy-Schwarz inequality implies

$$\Lambda(\mathbf{P}_{j,\nu} \mathbf{u}, \mathbf{u}) = \|\mathbf{P}_{j,\nu} \mathbf{u}\|_{\mathbf{H}(\text{div}; \Omega_{j,\nu})}^2 \leq \|\mathbf{P}_{j,\nu} \mathbf{u}\|_{\mathbf{H}(\text{div}; \Omega_{j,\nu})} \|\mathbf{u}\|_{\mathbf{H}(\text{div}; \Omega_{j,\nu})},$$

which is equivalent to  $\Lambda(\mathbf{P}_{j,\nu} \mathbf{u}, \mathbf{u}) \leq \|\mathbf{u}\|_{\mathbf{H}(\text{div}; \Omega_{j,\nu})}^2$ . This in turn yields the bound

$$\sum_{\nu \in \mathcal{N}_j} \Lambda(\mathbf{P}_{j,\nu} \mathbf{u}, \mathbf{u}) \leq \sum_{\nu \in \mathcal{N}_j} \|\mathbf{u}\|_{\mathbf{H}(\text{div}; \Omega_\nu)}^2 \leq \kappa \Lambda(\mathbf{u}, \mathbf{u}), \quad (47)$$

where  $\kappa$  is the maximum overlap of subdomains  $\Omega_{j,\nu}$ . In this 2D setting,  $\kappa = 4$ . Finally, using (46) and (47), we have

$$\Lambda([\mathbf{I} - R_j \Lambda_j] \mathbf{u}, \mathbf{u}) \geq (1 - \kappa \eta) \Lambda(\mathbf{u}, \mathbf{u}) > 0,$$

since  $\eta \in [0, \frac{1}{\kappa})$  implies that  $1 - \kappa \eta > 0$ . This is where our restrictions on the choice of  $\eta$  arises.

### 6.2. Verification of (38) for Symmetric Additive Relaxation Operator

To begin the verification of (38), keep in mind the equality in *Remark 2* given by

$$\eta \langle R_j^{-1} \mathbf{v}, \mathbf{v} \rangle = \inf_{\substack{\mathbf{v}_\nu \in \mathbf{MT}_{j,\nu} \\ \mathbf{v} = \sum_{\nu \in \mathcal{N}_j} \mathbf{v}_\nu}} \sum_{\nu \in \mathcal{N}_j} \Lambda(\mathbf{v}_\nu, \mathbf{v}_\nu). \quad (48)$$

With this at our disposal, we use the discrete Helmholtz decomposition to write

$$\mathbf{v} = \nabla_j s + \nabla^\perp w \in \mathbf{MT}_{0j},$$

for  $s \in S_j/\mathbf{R}$  and  $w \in W_{0j}$ . Denote  $\bar{\mathbf{v}} = \nabla_j s$  and  $\tilde{\mathbf{v}} = \nabla^\perp w$  and recall that  $\bar{\mathbf{v}} \perp \tilde{\mathbf{v}}$  in  $L^2$  and  $\mathbf{H}(\text{div})$ . This implies that  $\Lambda(\bar{\mathbf{v}}, \bar{\mathbf{v}}) + \Lambda(\tilde{\mathbf{v}}, \tilde{\mathbf{v}}) = \Lambda(\mathbf{v}, \mathbf{v})$ . The remainder of the proof proceeds by independently establishing the two inequalities,

$$\sum_{\nu \in \mathcal{N}_j} \Lambda(\tilde{\mathbf{v}}_\nu, \tilde{\mathbf{v}}_\nu) \leq C \Lambda(\mathbf{v}, \mathbf{v}) \quad (49)$$

and

$$\sum_{\nu \in \mathcal{N}_j} \Lambda(\bar{\mathbf{v}}_\nu, \bar{\mathbf{v}}_\nu) \leq C \Lambda(\mathbf{v}, \mathbf{v}), \quad (50)$$

for some decomposition of  $\tilde{\mathbf{v}}$  and  $\bar{\mathbf{v}}$  given by

$$\tilde{\mathbf{v}} := \sum_{\nu \in \mathcal{N}_j} \tilde{\mathbf{v}}_\nu \quad \text{and} \quad \bar{\mathbf{v}} := \sum_{\nu \in \mathcal{N}_j} \bar{\mathbf{v}}_\nu. \quad (51)$$

To define such a decomposition, we introduce a partition of unity,  $\{\theta_\nu\}_{\nu \in \mathcal{N}_j}$ , of  $\Omega$ . Such a partition of unity can be defined with the following properties:

$$\sum_{\nu \in \mathcal{N}_j} \theta_\nu = 1 \quad \text{and} \quad 0 \leq \theta_\nu \leq 1 \quad (52)$$

$$\|\nabla \theta_\nu\|_{L^\infty(\Omega_{j,\nu})} \leq K_0 h_{j-1}^{-1}, \quad (53)$$

where  $K_0$  is independent of the mesh. For example, from (14) we may use Hermite basis functions of the first kind to construct  $\theta_\nu$ . Hence, let  $\theta_\nu$  be the basis function in  $W_{0j}$  that has value one at node  $\nu$  and zero at every other node, and has derivative equal to zero at all nodes. It is easy to show that such a partition satisfies (52) and (53). The proof now continues by using this partition.

We begin with proving (49) by noting that  $\tilde{\mathbf{v}} = \nabla^\perp w$  for some  $w \in W_{0j}$ . Let  $w_\nu = \mathbf{I}_j^W(\theta_\nu w) \in W_{0j}$ , where  $\mathbf{I}_j^W$  is the nodal interpolant for  $W_j$ . Thus we have

$$\tilde{\mathbf{v}} = \nabla^\perp w = \sum_{\nu \in \mathcal{N}_j} \nabla^\perp w_\nu = \sum_{\nu \in \mathcal{N}_j} \tilde{\mathbf{v}}_\nu.$$

Note that  $\Lambda(\tilde{\mathbf{v}}_\nu, \tilde{\mathbf{v}}_\nu) = \|\nabla^\perp w_\nu\|^2 = |w_\nu|_1^2$ . In addition, recall that  $\Omega_{j,\nu}$  is the union of a number of elements  $T \in \mathcal{T}_h$ . We evaluate  $|w_\nu|_1^2$  only over  $T \in \mathcal{T}_h$  and apply an inverse estimate for  $W_j$  to obtain

$$|w_\nu|_{1,T}^2 = |\mathbf{I}_j^W(\theta_\nu w)|_{1,T}^2 \leq \frac{C}{h_j^2} \|\mathbf{I}_j^W(\theta_\nu w)\|_{0,T}^2, \quad (54)$$

where  $C$  is independent of the mesh. Because  $\theta_\nu w$  is the product of polynomials of degree six in  $x$  and  $y$  and  $\mathbf{I}_j^W$  interpolates to a lower-order polynomial, we have

$$\|\mathbf{I}_j^W(\theta_\nu w)\|_{0,T} \leq C \|\theta_\nu w\|_{0,T} \leq C \|w\|_{0,T}. \quad (55)$$

With (54) and (55), we get

$$|w_\nu|_{1,T}^2 \leq \frac{C}{h_j^2} \|w\|_{0,T}^2. \quad (56)$$

Summing over every  $T \in \mathcal{T}_h \cap \Omega_{j,\nu}$  yields

$$|w_\nu|_{1,\Omega_{j,\nu}}^2 \leq \frac{C}{h_j^2} \|w\|_{0,\Omega_{j,\nu}}^2,$$

which implies

$$\sum_{\nu \in \mathcal{N}_j} |w_\nu|_{1,\Omega}^2 \leq C \frac{\kappa}{h_j^2} \|w\|_{0,\Omega}^2,$$

where  $\kappa$  is the maximum overlap and  $C$  is independent of  $h_j$ . Recollecting inequality (41) of Lemma 6.2 and assuming that  $h_{j-1} = ph_j$  yields

$$\sum_{\nu \in \mathcal{N}_j} \Lambda(\tilde{\mathbf{v}}_\nu, \tilde{\mathbf{v}}_\nu) = \sum_{\nu \in \mathcal{N}_j} |w_\nu|_{1,\Omega}^2 \leq C \|\mathbf{v}\|_{\mathbf{H}(\text{div};\Omega)}^2 \leq C \Lambda(\mathbf{v}, \mathbf{v}),$$

where  $\kappa$  is absorbed into  $C$ . Consequently, inequality (49) has been proven.

The proof of (50) is similar, but it relies on the standard interpolation operator for  $\mathbf{MT}_j$ , which we shall denote by  $\Pi_j$ . Let  $\tilde{\mathbf{v}}_\nu := \Pi_j(\theta_\nu \bar{\mathbf{v}})$  such that  $\bar{\mathbf{v}} = \sum \tilde{\mathbf{v}}_\nu$ . Again, we separately consider the two terms that define inner product:  $\langle \cdot, \cdot \rangle$  and  $\langle \text{div} \cdot, \text{div} \cdot \rangle$ . Consider first the zeroth-order term. Again, because  $\theta_\nu \bar{\mathbf{v}}$  consists of polynomial of degree six in  $x$  and  $y$  and  $\Pi_j$  interpolates to a lower-order polynomial, we have

$$\|\tilde{\mathbf{v}}_\nu\|_{0,T}^2 = \|\Pi_j(\theta_\nu \bar{\mathbf{v}})\|_{0,T}^2 \leq C \|\theta_\nu \bar{\mathbf{v}}\|_{0,T}^2 \leq C \|\bar{\mathbf{v}}\|_{0,T}^2 \quad (57)$$

Taking a sum over  $T \in \mathcal{T}_j \cap \Omega_{j,\nu}$  yields

$$\|\tilde{\mathbf{v}}_\nu\|_{0,\Omega_{j,\nu}}^2 \leq C \|\bar{\mathbf{v}}\|_{0,\Omega_{j,\nu}}^2.$$

Taking the sum next over all  $\Omega_{j,\nu}$ , we get the final estimate

$$\sum_{\nu \in \mathcal{N}_j} \|\tilde{\mathbf{v}}_\nu\|_0^2 \leq \kappa C \|\bar{\mathbf{v}}\|_0^2, \quad (58)$$

where  $\kappa$  and  $C$  are independent of mesh size. Later we will refer to the product of  $\kappa$  and  $C$  as just  $C$ .

Consider next the higher-order term and the fact that

$$\langle \text{div} \mathbf{v}, \text{div} \mathbf{v} \rangle = \|\text{div} \mathbf{v}\|^2 \leq \sqrt{2} |\mathbf{v}|_1^2. \quad (59)$$

We can also express this relationship over  $T$  as

$$\|\text{div} \tilde{\mathbf{v}}_\nu\|_{0,T}^2 \leq \sqrt{2} |\tilde{\mathbf{v}}_\nu|_{1,T}^2.$$

With (56) in mind, which uses an inverse inequality, we recall that we can write

$$|\tilde{\mathbf{v}}_\nu|_{1,T}^2 \leq \frac{C}{h_{j-1}^2} \|\tilde{\mathbf{v}}\|_{0,T}^2,$$

for some constant  $C$ . Summing over every  $T \in \mathcal{T}_j \cap \Omega_{j,\nu}$  yields

$$\|\text{div} \tilde{\mathbf{v}}_\nu\|_{1,\Omega_{j,\nu}}^2 \leq \sqrt{2} |\tilde{\mathbf{v}}_\nu|_{1,\Omega_{j,\nu}}^2 \leq \frac{C}{h_j^2} \|\tilde{\mathbf{v}}\|_{0,\Omega_{j,\nu}}^2,$$

where  $\sqrt{2}$  is merged into  $C$ . Summing over every  $\Omega_{j,\nu}$  and applying Lemma 6.2 yields

$$\sum_{\nu \in \mathcal{N}_j} \|\operatorname{div} \bar{\mathbf{v}}_\nu\|_0^2 \leq C \frac{\kappa}{h_j^2} \|\bar{\mathbf{v}}\|_0^2 \leq C \|\mathbf{v}\|_{\mathbf{H}(\operatorname{div})}^2. \quad (60)$$

With (58) and (60) we have

$$\begin{aligned} \sum_{\nu \in \mathcal{N}_j} \Lambda(\bar{\mathbf{v}}_\nu, \bar{\mathbf{v}}_\nu) &= \sum_{\nu \in \mathcal{N}_j} \|\bar{\mathbf{v}}_\nu\|^2 + \|\operatorname{div} \bar{\mathbf{v}}_\nu\|^2 \\ &\leq C \Lambda(\mathbf{v}, \mathbf{v}). \end{aligned}$$

Hence, we have proved both (49) and (50) and therefore verified (38), which completes the proof. Note that proving (49) and (50) guarantees that the additive relaxation operator sufficiently reduces error orthogonal to the coarse grid, i.e. all high-frequency error components.

### 6.3. Verification of (37) and (38) for Symmetric Multiplicative Relaxation Operator

For the symmetric multiplicative relaxation operator, we define  $K_j = (I - \widehat{R}_j \Lambda_j)$ , the reduction in error from the operator defined by (33). With this definition, we set  $K_j^* K_j$  to be the reduction in the error from the symmetric multiplicative relaxation operator,  $\tilde{R}_j$ , which is produced by following a sweep of the nonsymmetric smoother with a sweep that goes over the vertices of the mesh in a reverse order. Here  $K_j^*$  is the adjoint with respect to the  $\Lambda(\cdot, \cdot)$  inner product. Note that  $K_j^* K_j$  is  $\Lambda(\cdot, \cdot)$ -symmetric; it is also positive definite since  $K_j^*$  is the  $\Lambda$ -conjugate of the nonsingular operator  $K_j$ . These results imply condition (37) is guaranteed for  $\tilde{R}_j$ .

To guarantee condition (38), we refer to a result from [1]. In this paper, the authors prove

$$\eta \langle \tilde{R}_j \mathbf{v}, \mathbf{v} \rangle \geq \kappa^{-2} \langle R_j \mathbf{v}, \mathbf{v} \rangle,$$

where  $\kappa$  is as previously defined. Because  $\kappa = 4$  for the subdomains  $\{\Omega_{j,\nu}\}$ , we can write

$$\langle R_j \mathbf{v}, \mathbf{v} \rangle \leq 16 \eta \langle \tilde{R}_j \mathbf{v}, \mathbf{v} \rangle, \quad \text{for all } \mathbf{v} \in \mathbf{MT}_j, \quad (61)$$

for the  $\mathbf{MT}$  elements. We subsequently use (61) to verify (38) for  $\tilde{R}_j$ .

Let  $\mathbf{v} = [\mathbf{I} - \mathbf{P}_{j-1}] \mathbf{u} \in \mathbf{MT}_j$ . As in the proof of Theorem 6.1, let  $\mathbf{v}$  be decomposed as  $\sum \mathbf{v}_\nu$ , for  $\mathbf{v}_\nu \in \mathbf{MT}_{j,\nu}$  in such a way as to satisfy

$$\sum_{\nu \in \mathcal{N}_j} \Lambda(\mathbf{v}_\nu, \mathbf{v}_\nu) \leq C \Lambda(\mathbf{v}, \mathbf{v}). \quad (62)$$

Then the sequence of inequalities follows:

$$\begin{aligned} (\tilde{R}_j^{-1} \mathbf{v}, \mathbf{v}) &= \sum_{\nu \in \mathcal{N}_j} \Lambda(\mathbf{P}_{j,\nu} \Lambda_j^{-1} \tilde{R}_j^{-1} \mathbf{v}, \mathbf{v}_\nu) \\ &\leq \left[ \sum_{\nu \in \mathcal{N}_j} \Lambda(\mathbf{P}_{j,\nu} \Lambda_j^{-1} \tilde{R}_j^{-1} \mathbf{v}, \Lambda_j^{-1} \tilde{R}_j^{-1} \mathbf{v}) \right]^{1/2} \left[ \sum_{\nu \in \mathcal{N}_j} \Lambda(\mathbf{v}_\nu, \mathbf{v}_\nu) \right]^{1/2} \\ &= \eta^{-1/2} (R_j \tilde{R}_j^{-1} \mathbf{v}, \tilde{R}_j^{-1} \mathbf{v})^{1/2} \left[ \sum_{\nu \in \mathcal{N}_j} \Lambda(\mathbf{v}_\nu, \mathbf{v}_\nu) \right]^{1/2}. \end{aligned}$$

We now use (61) and (62) to say

$$(\tilde{R}_j^{-1} \mathbf{v}, \mathbf{v}) \leq C (\tilde{R}_j^{-1} \mathbf{v}, \mathbf{v})^{1/2} \Lambda(\mathbf{v}, \mathbf{v})^{1/2},$$

which implies (38) for the symmetric multiplicative relaxation operator.

## 7. FINAL REMARKS

We have presented a method for both accurately discretizing and robustly solving variational problem (6). Although we provided a rigorous proof of convergence of the multigrid algorithm for the more difficult problem with  $\varepsilon = 0$  and fewer boundary conditions, theory that establishes convergence for all  $\varepsilon$  in  $(0, 1]$  remains an open problem. Numerical results imply that convergence factors improve as  $\varepsilon$  is increased. A possible extension of this work would be to establish a  $C^1$  finite element space on triangular meshes, construct a FE space  $\mathbf{MT}$  in a manner similar to section 3, and then a multigrid algorithm like that described in section 4. Another important extension is to see how this method performs for problems that have variable, and in particular, discontinuous  $\varepsilon$ .

## REFERENCES

1. Arnold DN, Falk RS, and Winther R. Preconditioning in  $H(\text{div})$  and applications. *Mathematics of Computation* **66**(219):957-984
2. Austin TM. Advances on a Scaled Least-Squares Method for the 3-D Linear Boltzmann Equation. *University of Colorado Thesis* University of Colorado: 2001.
3. Braess D. *Finite Elements* Cambridge University Press: Cambridge, 1997.
4. Bramble JH. *Multigrid Methods* Pitman Research Notes in Mathematics Series: 1993.
5. Brandt A. *Multigrid Techniques: 1984 Guide, with Applications to Fluid Dynamics* ISBN-3-88457-081-1; GMD-Studien Nr. 85: 1984.
6. Brenner SC and Scott LR. *The Mathematical Theory of Finite Element Methods* Springer: New York, 1994.
7. Brezzi F and Fortin M. *Mixed and Hybrid Finite Element Methods* Springer-Verlag: 1991.
8. Briggs WL, Henson VE, and McCormick SF. *A Multigrid Tutorial: Second Edition*
9. Girault V and Raviart P-A. *Finite Element Methods for Navier-Stokes Equations: Theory and Algorithms* Springer-Verlag: 1986. SIAM: Philadelphia, 2001.
10. Hiptmair R and Hoppe RHW. Multilevel methods for mixed finite elements in three dimensions. *Numerische Mathematik* **82**:253-279.
11. Manteuffel TA, Ressel K, and Starke G. A boundary functional for the least-squares finite element solution of neutron transport problems. *SIAM Journal on Numerical Analysis* **37**:556-586.
12. Mardal KA, Tai XC, and Winther R. A robust finite element method for Darcy-Stokes Flow. *SIAM Journal on Numerical Analysis* **40**(5):1605-1631
13. Vassilevski PS and Wang J. Multilevel iterative methods for mixed finite element discretizations of elliptic problems. *Numerische Mathematik* **63**(4):503-520.